

# End-group analysis of vinyl polyperoxides by MALDI-TOF-MS, FT-IR technique and thermochemical calculations

A.K. Nanda<sup>a,\*</sup>, K. Ganesh<sup>a</sup>, K. Kishore<sup>a</sup>, M. Surinarayanan<sup>b</sup>

<sup>a</sup>Department of Inorganic and Physical Chemistry, Indian Institute of Science, Bangalore 560012, India

<sup>b</sup>Central Leather Research Institute, Adyar, Chennai, India

Received 4 October 1999; received in revised form 14 January 2000; accepted 19 January 2000

## Abstract

A first comprehensive investigation has been made to unequivocally analyze the end groups of two vinyl polyperoxide polymers namely, poly( $\alpha$ -methylstyrene peroxide), and poly(methylmethacrylate peroxide), using matrix-assisted laser desorption ionization-time of flight-mass spectrometry, Fourier transform-infra red techniques and thermochemical calculations. In both the polymers, the end groups formed due to chain transfer reactions were found in large concentrations. Detail mechanism of the formation of end groups has been presented. © 2000 Elsevier Science Ltd. All rights reserved.

**Keywords:** End groups analysis; Polyperoxides; MALDI-TOF-MS

## 1. Introduction

Although polymer properties are determined largely by the backbone structure, the end groups also significantly influence the bulk properties of the polymers. For example, thermal stabilities are profoundly affected by the nature of the end groups [1–3]. Precise knowledge about the end groups also helps in understanding the mechanism of polymerization particularly the termination and chain transfer reactions. Generally in most polymers, depending upon the nature of the initiating species, the end groups are established a priori. However, in relatively unstable polymeric systems the identification of the end groups is rendered difficult due to the degradation of chains during polymerization itself. In such situations the end groups are likely to change and are mostly governed by the reaction conditions. Vinyl polyperoxides are striking examples of this type where the polymers degrade in a complex fashion during polymerization [4,5] and, as a result, precise establishment of the end groups has remained elusive for a long time.

The only detailed attempt on the end groups analysis of a polyperoxide viz. poly(styrene peroxide) (PSP) has been made by Cais and Bovey using <sup>13</sup>C NMR spectroscopy

[6]. Although it does give a fair amount of insight on the groups, a few assignments could not be fully established. In view of the current resurgence of polyperoxide as fuels [7] and initiators [8,9], it has become imperative to establish the nature of the end groups unequivocally for a better understanding of their physico-chemical behavior.

Traditionally, methods like nuclear magnetic resonance (NMR), ultraviolet–visible (UV–VIS) and infrared (IR) spectroscopies, elemental analysis techniques were employed to determine the mode of chain termination in free radical oxidative polymerization. Unfortunately, precise identification and quantification of chain ends are not always possible with the above methods.

In the present study, we have used Matrix-assisted laser desorption ionization-time of flight-mass spectrometry (MALDI-TOF-MS) to determine the end groups accurately of two polyperoxide polymers namely poly( $\alpha$ -methylstyrene peroxide) (PMSP) and poly(methylmethacrylate peroxide) (PMMAP). MALDI-TOF-MS is a recently introduced [10,11] soft ionization technique that allows desorption and ionization of very large molecules even if in complex mixtures, such as the wide molecular weight distribution (MWD) present in synthetic and natural macromolecules [12,13]. With MALDI-TOF-MS, the identification of end groups could be made accurately and this is the most sought after technique recently for the mass analysis of synthetic polymers [14,15].

\* Corresponding author. Tel.: + 91-080-3092382; fax: + 91-080-3341683.

E-mail address: ajaya@ipc.iisc.ernet.in (A.K. Nanda).

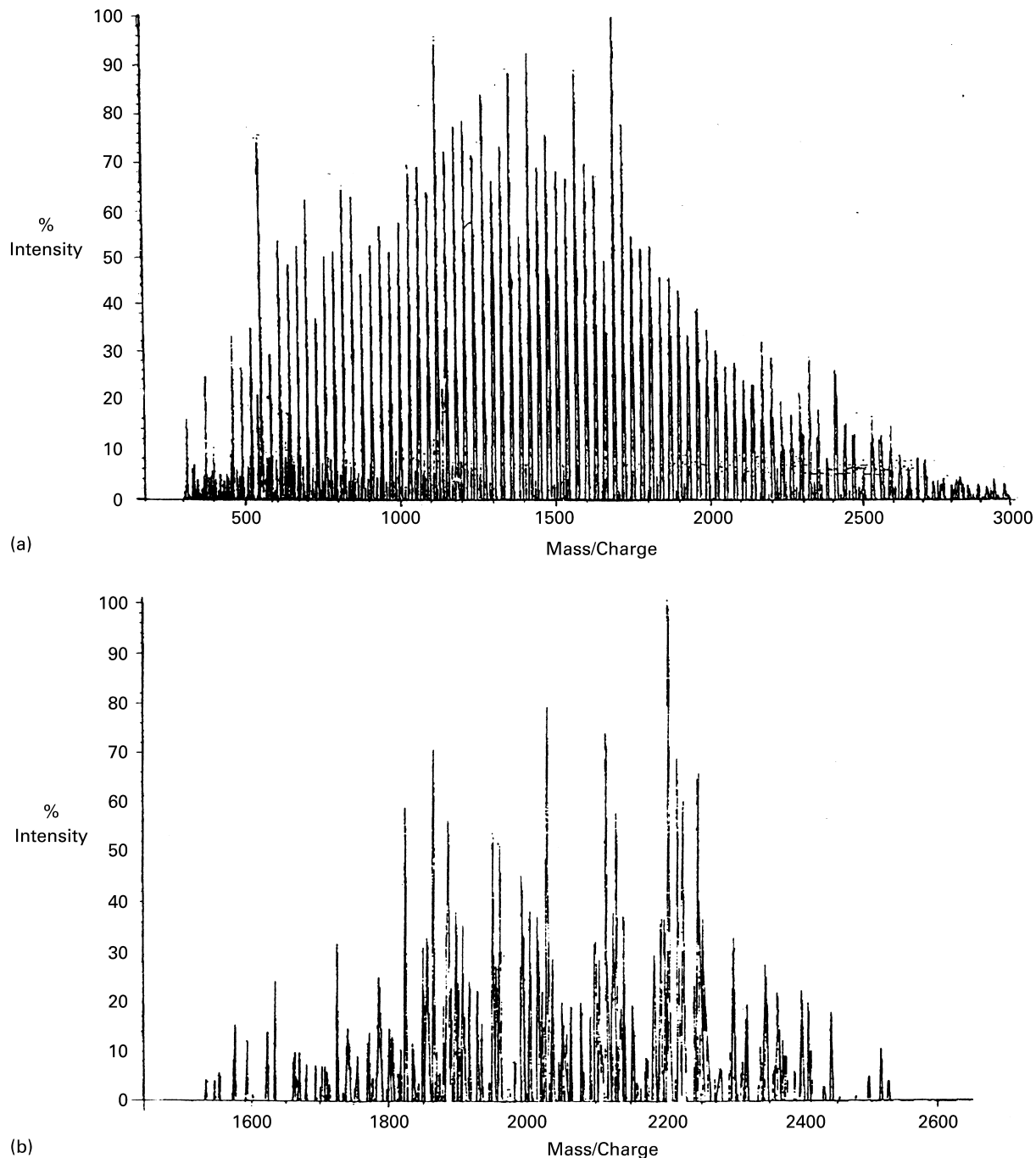


Fig. 1. MALDI-TOF-MS of: (a) PMSP; and (b) PMMAP.

## 2. Experimental section

### 2.1. Polymerization

$\alpha$ -Methylstyrene (AMS), methylmethacrylate (MMA) and Azobis(isobutyronitrile) (AIBN) were purified by usual procedures and oxidative polymerization was carried out in 300 ml Parr reactor [16]. The preparation of PMSP and PMMAP have been reported elsewhere [4,5,16].

### 2.2. Molecular weight analysis

The number average molecular weight ( $M_n$ ) and the weight average molecular weight ( $M_w$ ) were estimated by GPC (Waters HCL/GPC 244, with RI detector) using THF as solvent. The GPC instrument was calibrated using polystyrene as standards. The  $M_n$  and  $M_w/M_n$  of PMSP are found to be 2500 and 1.61, respectively [9]. Similarly, for PMMAP, we observed  $M_n$  to be 1800 and  $M_w/M_n$  is 1.58 [9].

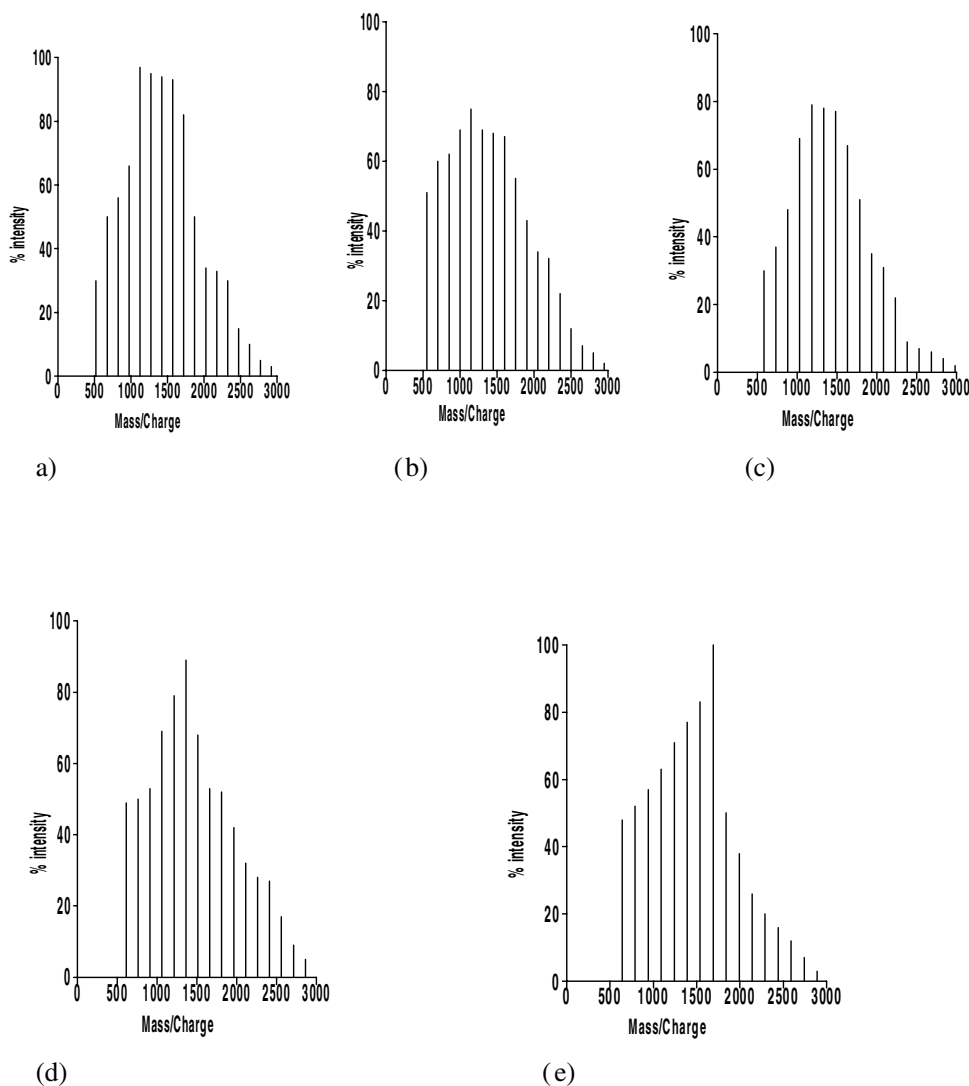


Fig. 2. Simulated individual MALDI-TOF-MS of PMSP having different end groups.

### 2.3. MALDI-TOF-MS

Mass spectrometry was carried out on a Kratos Kompact III MALDI-TOF MS (Kratos, Manchester, UK), incorporating a 337 nm nitrogen laser with a 3 ns pulse duration and an electron multiplier detector. The instrument was operated in the positive ion reflectron mode with an accelerating potential of +20 kV. The mass scale was calibrated using bovine insulin. For each sample the spectrum was averaged over 180 laser shots. Careful modification of the laser power was required to operate at the threshold energy.

### 2.4. MALDI-TOF sample preparation

The matrix and cation used for PMSP were 2,5-dihydroxybenzoic acid (Aldrich) and  $\text{Na}^+$ , respectively. Polyperoxide solutions in THF were made up at a concentration of 0.1 mg of polyperoxide per ml. The polymer solutions (0.5  $\mu\text{l}$ ) were

deposited on the matrix (or mixed with the matrix) and allowed to dry.

### 2.5. FT-IR measurements

The FT-IR spectra of PMSP and PMMAP were recorded on a Fourier Transform Bio-rad (FTS7) spectrophotometer.

## 3. Results and discussion

### 3.1. MALDI-TOF-MS analysis

Determination of end groups of polymers using MALDI-TOF-MS technique have been reported elsewhere [14,15]. In brief, for MALDI-TOF-MS analysis, the polymer is mixed with the matrix. The matrix, which has a resonance absorption at the laser wave length, absorbs the laser energy and causes rapid heating of the matrix for the polymer to be vaporized. The unique advantage of MALDI-TOF-MS

Table 1  
Structural assignments of different end groups present in PMSP deduced from MALDI-TOF-MS data

a	$\text{HOCH}_2\text{O}-(\text{CH}_2-\overset{\text{CH}_3}{\underset{\text{Ph}}{\text{C}}}-\text{OO})_n-\text{H} + \text{Na}^+$
b	$\text{HOCH}_2\text{O}-(\text{CH}_2-\overset{\text{CH}_3}{\underset{\text{Ph}}{\text{C}}}-\text{OO})_n-\text{CH}_2\text{OH} + \text{Na}^+$
c	$\text{HOCO}-(\overset{\text{CH}_3}{\underset{\text{Ph}}{\text{C}}}-\text{CH}_2-\overset{\text{CH}_3}{\underset{\text{Ph}}{\text{C}}}-\text{OO})_n-\text{H} + \text{Na}^+$
d	$\text{HOCO}-(\overset{\text{CH}_3}{\underset{\text{Ph}}{\text{C}}}-\text{CH}_2-\overset{\text{CH}_3}{\underset{\text{Ph}}{\text{C}}}-\text{OO})_n-\overset{\text{CH}_3}{\underset{\text{Ph}}{\text{C}}}-\text{COH} + \text{Na}^+$
e	$\text{HOCH}_2\text{O}-(\text{CH}_2-\overset{\text{CH}_3}{\underset{\text{Ph}}{\text{C}}}-\text{OO})_n-\overset{\text{CH}_3}{\underset{\text{Ph}}{\text{C}}}-\text{COH} + \text{Na}^+$
or	$\text{HOCO}-(\overset{\text{CH}_3}{\underset{\text{Ph}}{\text{C}}}-\text{CH}_2-\overset{\text{CH}_3}{\underset{\text{Ph}}{\text{C}}}-\text{OO})_n-\text{CH}_2\text{OH} + \text{Na}^+$
f	$\text{CH}_3\overset{\text{CN}}{\underset{\text{C}}{\text{C}}}-\text{OO}-\text{CH}_2-\overset{\text{CH}_3}{\underset{\text{Ph}}{\text{C}}}-\text{OOH} + \text{Na}^+$
g	$\text{H}-\overset{\text{O}}{\parallel}{\text{C}}-\text{OO}-\text{CH}_2-\overset{\text{CH}_3}{\underset{\text{Ph}}{\text{C}}}-\text{OOH} + \text{Na}^+$

method lies in the matrix dissipating the heat energy created by the laser rapidly and hence the polymer vaporizes with almost no decomposition and detected. By using this technique, many polymers have been studied [12,13,17–19].

MALDI-TOF-MS spectrum of PMSP is given in Fig. 1(a). The matrix used is 2,5-dihydroxy benzoic acid and doped with NaCl to get the spectrum. Hence, each peak is observed as a  $\text{Na}^+$  adduct [20].

Fig. 1(a) comprises of total distribution of all PMSP chains having different end groups. In order to simplify and separate individual PMSP chains having specific end groups, computational simulation using the data from Fig. 1(a) has been made and all the individual distributions are presented in Fig. 2. We used Origin software, version 6.0 available in Microsoft Internet Explorer for the simulation experiment. The structural assignments corresponding to specific end groups are displayed in Tables 1 and 2.

Among the seven structures identified (Table 1), structures (a–e) have been found to form in greater concentrations while the AIBN fragment (structure f) and formyl fragment (structure g) presenting as the end group is observed in smaller amounts.

To further substantiate the MALDI-MS data, we have carried out the FT-IR analysis of PMSP (Fig. 3(a)). The broad absorption found between  $3500\text{--}3000\text{ cm}^{-1}$  corresponds to both  $-\text{OH}$  and  $-\text{OOH}$  end groups [21]. Since the nitrile peak absorption at  $2215\text{ cm}^{-1}$  is absent, it corroborates the MALDI-TOF-MS results that the AIBN end groups are present in smaller amounts. Based on the MALDI-TOF-MS and FT-IR data on the identification of different end groups, its mechanism of formation (Scheme 1) is discussed below.

### 3.2. Mechanism of polymerization

The mechanism of polymerization of PMSP has been adduced in Scheme 1. Initially, AIBN initiates the polymerization of PMSP and hence form the end groups (Eqs. (1)–(3)). It is to be noted here that similar to all polyperoxides, PMSP also undergoes degradation during polymerization forming acetophenone and formaldehyde as the degradation products (Eq. (4)). This explains as to why in the MALDI analysis we did not detect the AIBN fragment as end groups in larger proportions. During the propagation step there is always excess oxygen, besides the peroxy radicals being more stable than the alkyl radical, almost all the growing chain at any point of time will have a peroxide radical (Eq. (3)). The termination process then occurs by the chain transfer of hydrogen from formaldehyde to the propagating peroxy radical forming the  $-\text{OOH}$  end groups (Eq. (5)). The resultant formyl radical thus generated subsequently reacts with oxygen forming the formyl peroxy radical which further initiate the polymerization (Eq. (6)). It is to be noted here that formaldehyde is a good chain transfer agent for the radical polymerization of vinyl monomers [22].

The formation of acetophenone and formaldehyde is known to proceed to the cleavage of  $\text{O}-\text{O}$  linkage following by unzipping (Eq. (7)). The alkoxy radicals thus formed, apart from unzipping can also react with formaldehyde forming the  $-\text{OH}$  chain ends (Eqs. (7) and (8)). Eqs. (8) and (9) represent various radical recombination reactions forming the other type of hydroxyl end groups. The occurrence of such radical recombination reaction (Eq. (9)) is highly kinetically favored due to  $0\text{ kcal/mol}$  activation energy [23].

Although the formation of hydroxyl and hydroperoxy end groups are well established, the counter part, i.e. the formyl end groups has not been observed in larger proportions. We also found this discrepancy in the fast atom bombardment mass spectrometry (FABMS) analysis of PMMAP [21].

### 4. Thermochemical studies

To further understand the mechanism of polymerization, we have performed computational calculation on the heats of formation ( $\Delta H_f^0$ ) of various neutral species and radicals. Here, we have considered only the model radicals in place

Table 2  
MALDI-TOF-MS analysis results of PMSP

n	Structure a			Structure b			Structure c			Structure d			Structure e			Structure f			Structure g		
	Measd	Calcd	Intensity (%)	Measd	Calcd	Intensity (%)	Measd	Calcd	Intensity (%)	Measd	Calcd	Intensity (%)	Measd	Calcd	Intensity (%)	Measd	Calcd	Intensity (%)	Measd	Calcd	Intensity (%)
2							581.7	580.9	30												
3	521.0	520.9	30	550.8	550.9	51	731.0	730.9	37	610.8	610.9	49	641.0	640.9	48	574.1	574.0	9.1			
4	671.2	670.9	50	701.1	700.9	60	880.5	880.9	48	760.8	760.9	50	790.5	790.4	52	724.1	724.0	8.2			
5	821.1	820.9	56	850.8	850.9	62	1031.1	1030.9	69	910.8	910.9	53	940.7	940.9	57	874.2	874.0	4.5			
6	970.6	970.9	66	1001.3	1000.9	69	1181.7	1180.9	79	1060.9	1060.9	69	1091.7	1090.9	63	1023.9	1024.0	6.6	985.0	984.9	11.2
7	1120.3	1120.9	97	1150.8	1150.9	75	1331.1	1330.9	78	1211.5	1210.9	79	1241.1	1240.9	71	1174.1	1174.0	5.7	1134.9	1134.9	22.8
8	1271.4	1270.5	95	1300.9	1300.9	69	1480.0	1480.9	77	1360.8	1360.9	89	1390.7	1390.9	77	1324.2	1324.0	4.7	1285.1	1284.9	5.7
9	1420.5	1420.9	94	1451.1	1450.9	68	1631.7	1630.9	67	1511.2	1510.9	68	1541.0	1540.9	83				1435.1	1434.9	
10	1570.4	1570.9	93	1601.6	1600.9	67	1781.2	1780.9	51	1661.0	1660.9	53	1691.1	1690.9	100						
11	1721.2	1720.9	82	1751.6	1750.9	55	1931.1	1930.9	35	1810.2	1810.9	52	1841.4	1840.9	50						
12	1871.1	1870.9	50	1900.8	1900.9	43	2081.5	2080.9	31	1961.1	1960.9	42	1991.0	1990.9	38						
13	2021.1	2020.9	34	2050.8	2050.9	34	2230.5	2230.9	22	2111.4	2110.9	32	2140.7	2140.9	26						
14	2170.8	2170.9	33	2200.5	2200.9	32	2380.6	2380.9	9	2260.6	2260.9	28	2140.7	2140.9	26						
15	2321.6	2320.9	30	2351.7	2350.9	22	2530.2	2530.9	7	2410.8	2410.9	27	2441.5	2440.9	16						
16	2471.7	2470.9	15	2501.0	2500.9	12	2680.8	2680.9	6	2560.7	2560.9	17	2590.9	2590.9	12						
17	2621.0	2620.9	10	2650.8	2650.9	7	2831.5	2830.9	4	2710.8	2710.9	9	2741.0	2740.9	7						
18	2771.0	2770.9	5	2801.0	2800.9	5	2981.4	2980.9	2	2680.8	2680.9	5	2891.0	2890.9	3						
19	2921.0	2920.9	3	2950.8	2950.9	2				2680.8	2680.9	5	2891.0	2890.9	3						

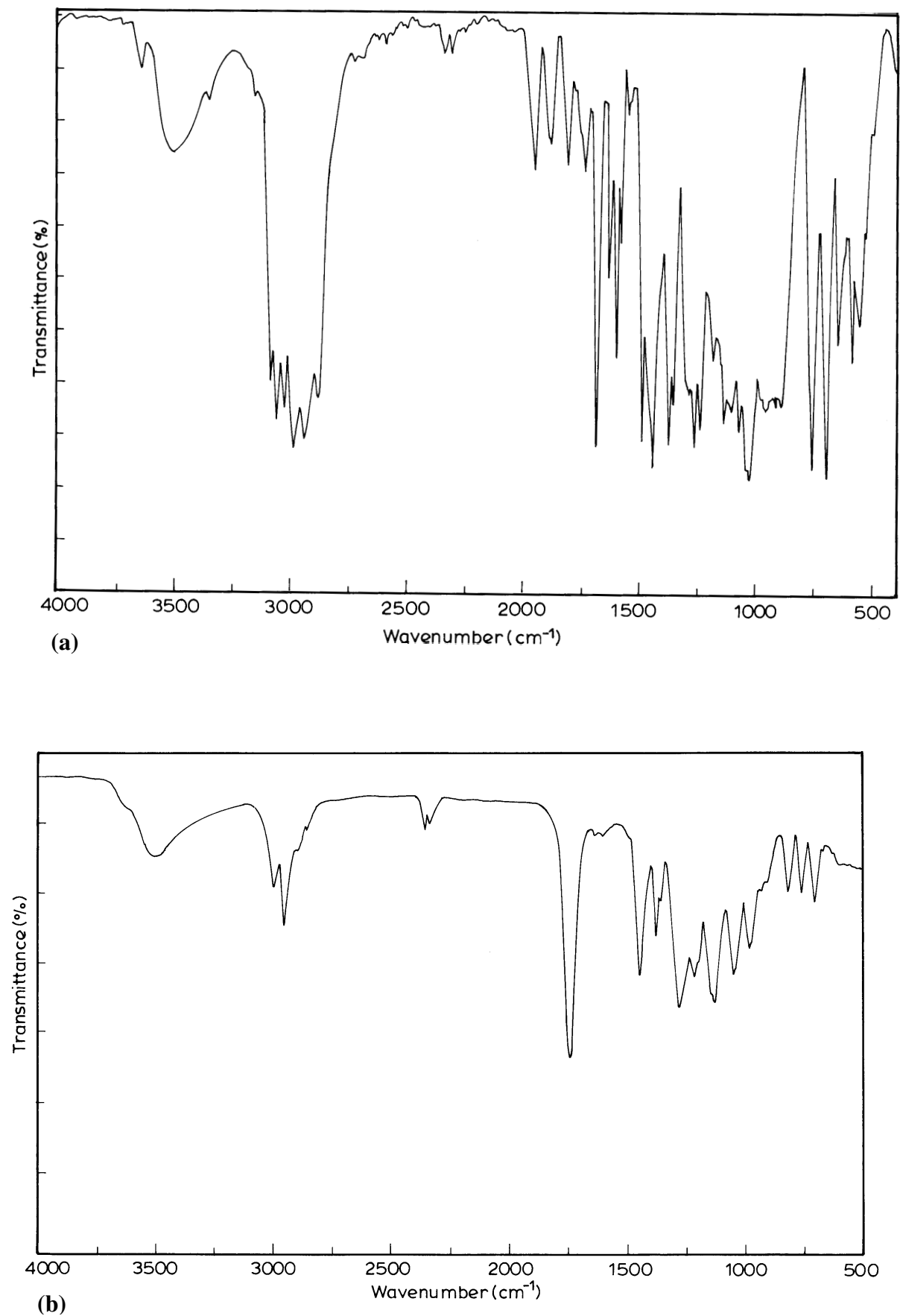
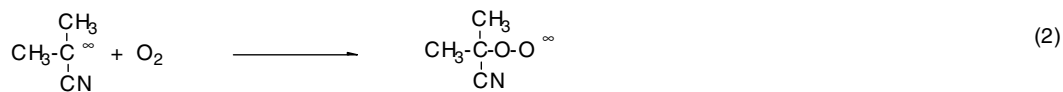
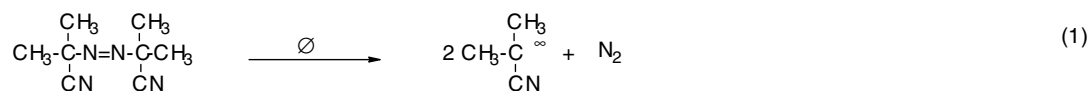
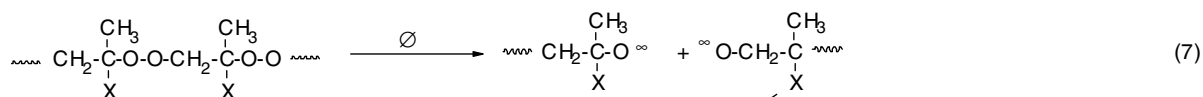
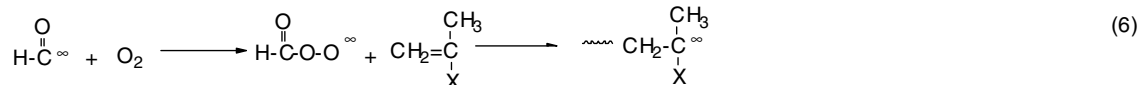
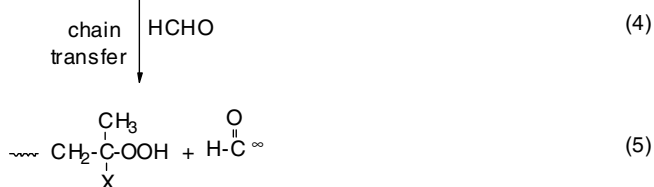
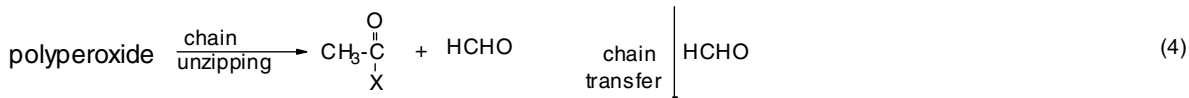
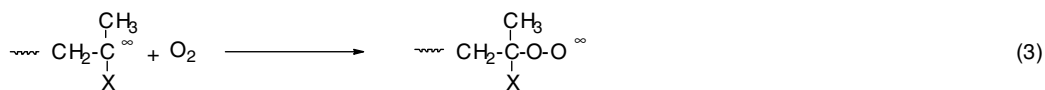


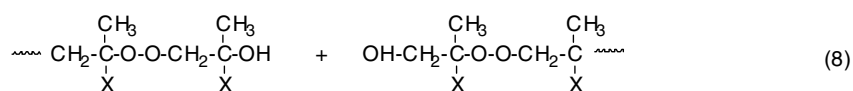
Fig. 3. FT-IR spectrum of: (a) PMSP; and (b) PMMAP.

initiation

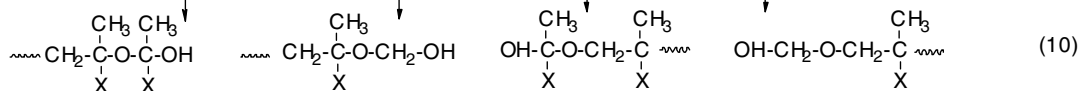
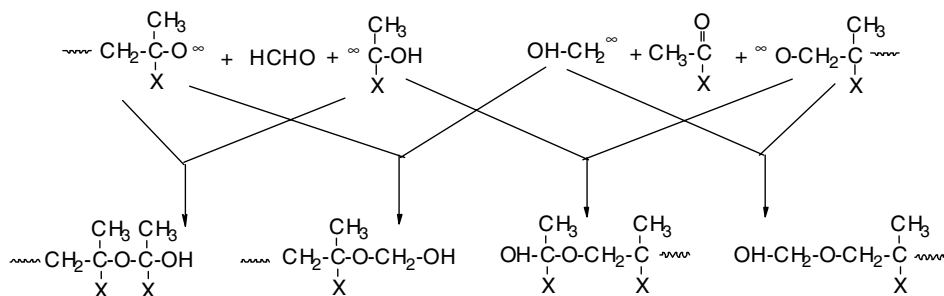
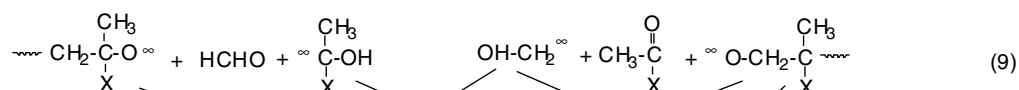


propagation



$$\begin{array}{c} \text{HCHO} \\ | \\ \text{chain transfer} \end{array}$$


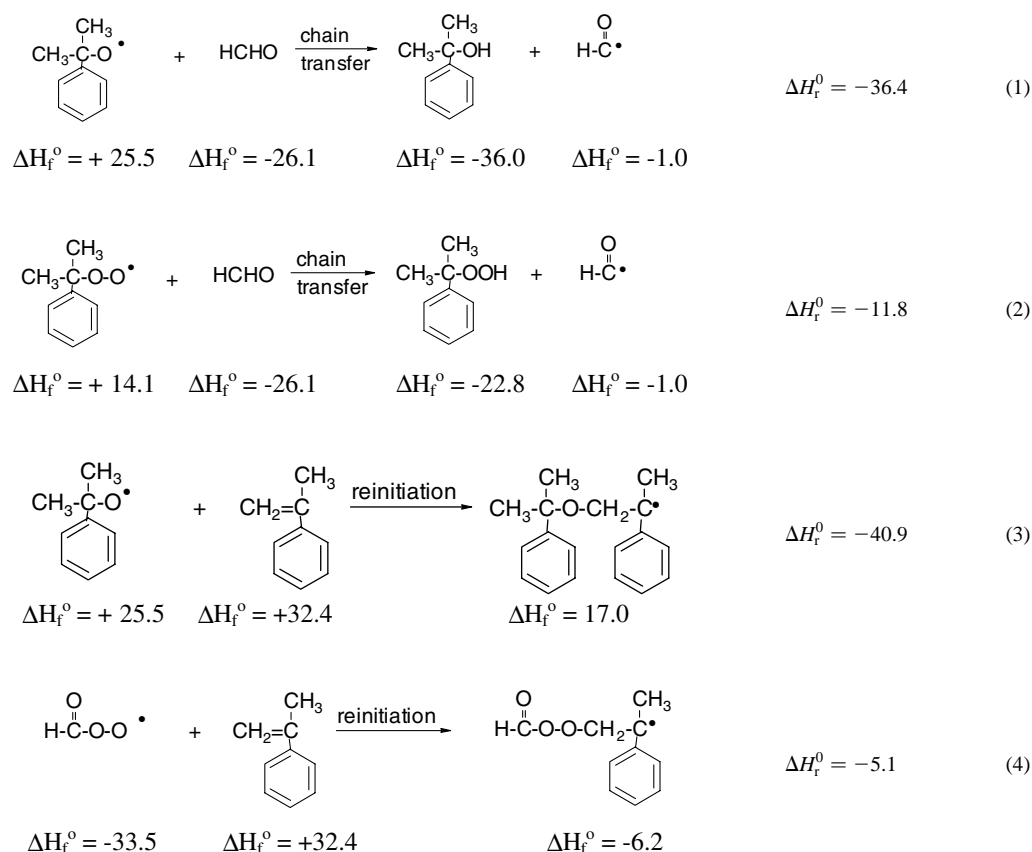
$$\begin{array}{c} \text{chain unzipping} \\ \downarrow \end{array}$$

$$\begin{array}{c} \text{chain unzipping} \\ \downarrow \end{array}$$
Scheme 1. Mechanism of polymerization of PMSPCX = C<sub>6</sub>H<sub>5</sub> and PMMAP (X = COOCH<sub>3</sub>).

of actual macro radicals. The commercial semiempirical program packages, MOPAC and VAMP version 6.0 were used for all computations [24,25]. The geometry of all the radicals were fully optimized using AM1 Hamiltonian.

We have considered here four possible model reactions (Table 3) and compared the heats of reaction ( $\Delta H_f^0$ ). It appears that the chain transfer reaction to formaldehyde (Eqs. (1) and (2)) and reinitiation by alkoxy radical

Table 3  
Thermochemical calculations of PMSP (all the enthalpy values are in kcal/mol)



(Eq. (3)) are more preferred (due to high negative  $\Delta H_r^0$  value) over reinitiation by dormant formyl peroxy radical (Eq. (4)). The reactivity data obtained here clearly explains as to why formyl end groups are not observed in high concentrations. Besides, the calculations also revealed that the reinitiation is mostly due to alkoxy radicals (Eq. (3)) in Table 3).

## 5. PMMAP

Fig. 1(b) and Table 4 represent MALDI-TOF-MS and the individual structures of PMMAP corresponding to different peaks, respectively. Similar to PMSP, here also, formyl and the AIBN fragment end groups ( $v$  and  $vi$  of Table 4) are present in lower concentrations.

FT-IR spectrum of PMMAP (Fig. 3(b)) also corroborates the MALDI-TOF-MS data by showing broad absorption between at  $3200\text{--}3500\text{ cm}^{-1}$  corresponding to  $-\text{OH}$  and  $-\text{OOH}$  end groups [21].

Table 5 explains the heat of various model reactions representing the PMMAP polymerization. Similar to PMSP, PMMAP also shows that the formation of hydroxyl

groups is more favored followed by the hydroperoxide groups. Further, the reinitiation due to alkoxy radicals appears to be mostly preferred over the same by formyl peroxy radicals.

The mechanism of polymerization of PMMAP, based on MALDI-TOF-MS, FT-IR and thermochemical calculations suggest that it follows similar to PMSP pathway (Scheme 1).

## 6. Conclusions

Based on the MALDI-TOF-MS, FT-IR and thermochemical calculations of PMSP and PMMAP, the following conclusions may be drawn.

1. In both the polymers, the AIBN and formyl end groups are present in smaller concentrations.
2. Both the polyperoxides degrade during polymerization and chain transfer to the degraded product occurs predominantly, hence the polymers mostly have the end groups generated during the chain transfer reactions.
3. Thermochemical calculations using the  $\Delta H_r^0$  data clearly



Table 4  
MALDI-TOF-MS analysis results of PMMAP

Structures	Molecular ions ( $m/z$ ) of $n$							
	11	12	13	14	15	16	17	18
(i) $\text{HO}-\text{CH}_2\text{O}-\left(\text{CH}_2-\overset{\text{CH}_3}{\underset{\text{COOCH}_3}{\text{C}}}-\text{O}-\text{O}\right)_n\text{H}+\text{Na}^+$	Measd Calcd Intensity	1654.5 1654.9 12	1787.1 1786.9 26	1918.2 1918.2 37	2050.6 2050.9 22	2183.7 2182.9 42	2314.5 2314.9 22	2446.7 2446.9 10
(ii) $\text{HO}-\text{CH}_2\text{O}-\left(\text{CH}_2-\overset{\text{CH}_3}{\underset{\text{COOCH}_3}{\text{C}}}-\text{O}-\text{O}\right)_n\text{CH}_2\text{OH}+\text{Na}^+$	Measd Calcd Intensity	1685.9 1685.4 10	1817.6 1817.4 62	1950.2 1949.4 56	2081.3 2081.4 35	2213.9 2213.4 32	2345.6 2345.9 28	2477.2 2477.4 12
(iii) $\text{HO}-\overset{\text{CH}_3}{\underset{\text{COOCH}_3}{\text{C}}}-\text{O}-\left(\text{CH}_2-\overset{\text{CH}_3}{\underset{\text{COOCH}_3}{\text{C}}}-\text{O}-\text{O}\right)_n\text{H}+\text{Na}^+$	Measd Calcd Intensity	1595.0 1594.9 8	1726.5 1726.9 32	1859.1 1859.9 72	2123.3 2122.9 60	2254.3 2254.9 41	2387.3 2386.9 28	2518.3 2518.9 12
(iv) $\text{HO}-\overset{\text{CH}_3}{\underset{\text{COOCH}_3}{\text{C}}}-\text{O}-\left(\text{CH}_2-\overset{\text{CH}_3}{\underset{\text{COOCH}_3}{\text{C}}}-\text{O}-\text{O}\right)_n\text{CH}_2\text{OH}+\text{Na}^+$	Measd Calcd Intensity	1625.1 1624.9 15	1756.9 1756.9 18	1889.2 1888.9 57	2021.3 2022.9 84	2152.6 2152.9 25	2285.1 2284.9 15	2417.2 2416.9 10
(v) $\text{CHO}-\left(\text{O}-\text{O}-\text{CH}_2-\overset{\text{CH}_3}{\underset{\text{COOCH}_3}{\text{C}}}\right)_n-\text{O}-\text{H}+\text{Na}^+$	Measd Calcd Intensity	1668.9 1668.9 12	1801.1 1800.9 16	1933.1 1932.9 25	2064.9 2064.9 27	2196.6 2196.9 40	2328.7 2328.9 13	2461.1 2460.9 2
(vi) $\text{CH}_3-\overset{\text{CH}_3}{\underset{\text{CN}}{\text{C}}}-\text{O}-\left(\text{O}-\text{O}-\text{CH}_2-\overset{\text{CH}_3}{\underset{\text{COOCH}_3}{\text{C}}}\right)_n-\text{O}-\text{H}+\text{Na}^+$	Measd Calcd Intensity	1708.1 1708.0 8	1839.9 1840.0 33	1971.9 1972.0 35	2104.6 2104.0 31	2235.9 2236.0 26	2367.9 2368.0 12	2500.6 2500.0 3

Table 5  
Thermochemical calculations of PMMAP (all the enthalpy values are in kcal/mol)

$\text{CH}_3-\overset{\text{CH}_3}{\underset{\text{COOCH}_3}{\text{C}}}-\text{O}^\bullet + \text{H}-\overset{\text{O}}{\parallel}{\text{C}}-\text{H} \longrightarrow \text{CH}_3-\overset{\text{CH}_3}{\underset{\text{COOCH}_3}{\text{C}}}-\text{O}-\text{H} + \text{H}-\overset{\text{O}}{\parallel}{\text{C}}^\bullet$	-34.1	(1)
$\text{CH}_3-\overset{\text{CH}_3}{\underset{\text{COOCH}_3}{\text{C}}}-\text{O}-\text{O}^\bullet + \text{H}-\overset{\text{O}}{\parallel}{\text{C}}-\text{H} \longrightarrow \text{CH}_3-\overset{\text{CH}_3}{\underset{\text{COOCH}_3}{\text{C}}}-\text{O}-\text{O}-\text{H} + \text{H}-\overset{\text{O}}{\parallel}{\text{C}}^\bullet$	-12.0	(2)
$\text{CH}_3-\overset{\text{CH}_3}{\underset{\text{COOCH}_3}{\text{C}}}-\text{O}^\bullet + \text{CH}_2=\overset{\text{CH}_3}{\underset{\text{COOCH}_3}{\text{C}}} \longrightarrow \text{CH}_3-\overset{\text{CH}_3}{\underset{\text{COOCH}_3}{\text{C}}}-\text{O}-\text{CH}_2-\overset{\text{CH}_3}{\underset{\text{COOCH}_3}{\text{C}}}^\bullet$	-44.1	(3)
$\text{H}-\overset{\text{O}}{\parallel}{\text{C}}-\text{O}-\text{O}^\bullet + \text{CH}_2=\overset{\text{CH}_3}{\underset{\text{COOCH}_3}{\text{C}}} \longrightarrow \text{H}-\overset{\text{O}}{\parallel}{\text{C}}-\text{O}-\text{O}-\text{CH}_2-\overset{\text{CH}_3}{\underset{\text{COOCH}_3}{\text{C}}}^\bullet$	-11.1	(4)

explained as to why the formyl and AIBN fragments are present in less concentration.

In a nutshell, although the end groups formed in vinyl polyperoxides are very complex which depends on a host of parameters such as structure of monomers, chain transfer characteristic of degradable products, etc. we observe a common phenomena of initiator (AIBN) bearing end groups to occur in less concentration.

## References

- [1] Yoo Y, Kalic S, Mcgrath JE. *Polym Prepr (Am Chem Soc Div Polym Chem)* 1987;28(1):272.
- [2] Yoo Y, Kilic S, Mcgrath JE. *Polym Prepr (Am Chem Soc Div Polym Chem)* 1987;28(2):358.
- [3] Billmeyer Jr. FW. *Textbook of polymer science*. New York: Wiley, 1984.
- [4] Kishore K, Paramasivam S, Sandhya TE. *Macromolecules* 1996;29:6973.
- [5] Jayaseheran J, Kishore K. *Macromolecules* 1997;30:3985.
- [6] Cais RE, Bovey FA. *Macromolecules* 1977;10:169.
- [7] Kishore K, Mukundan T. *Nature* 1986;324:130.
- [8] Shamugananda Murthy K, Kishore K, Krishnamohan V. *Macromolecules* 1994;27:7109.
- [9] Kishore K, Shamugananda Murthy K. Oxygen copolymerization: the vinyl polyperoxides. In: Salamone JC, editor. *Polymeric materials encyclopedia: synthesis, properties and applications*, vol. II. Boca Raton, FL: CRC Press, 1996. p. 8378.
- [10] Karas M, Hillenkamp F. *Anal Chem* 1988;60:2299.
- [11] Hillenkamp F, Karas M, Beavis RC, Chait BT. *Anal Chem* 1991; 63:1193A.
- [12] Bahr U, Deppe A, Karas M, Hillenkamp F, Giessman U. *Anal Chem* 1992;64:2866.
- [13] Mantaudo G, Mantaudo MS, Puglisi C, Samperi F. *Macromolecules* 1995;28:4562.
- [14] Zammit MD, Davis TP, Haddleton DM, Suddaby KG. *Macromolecules* 1997;30:1915.
- [15] Maloney DR, Hunt KH, Lloyd PM, Muir AVG, Richards SN, Derrick PJ, Haddleton DM. *J Chem Soc; Chem Commun* 1995:561.
- [16] Shamugananda Murthy K, Kishore K, Krishnamohan V. *Macromolecules* 1996;29:4853.
- [17] Freitag R, Baltes T, Eggert M. *J Polym Sci, Polym Chem Ed* 1994; 32:3019.
- [18] Burger HM, Muller H, Seebach D, Bornsen KO, Schar M, Widmer HM. *Macromolecules* 1993;26:4783.
- [19] Chan PK, Wang Y, Hay AS, Hronowski XL, Cotter RJ. *Macromolecules* 1995;28:6705.
- [20] Zammit MD, Davis TP, Haddleton DM, Suddaby KG. *Macromolecules* 1997;30:1915.
- [21] Ganesh K, Paramasivam S, Kishore K. *Polym Bull* 1996;37:785.
- [22] Brandrup J, Immergut EH. *Polymer handbook*. New York: Wiley, 1975.
- [23] Mogilevich MM. *Russ Chem Rev* 1979;48(2):199.
- [24] Dewar MJS, Zeobisch EG, Healy EF, Stewart JJP. *J Am Chem Soc* 1985;107:3902.
- [25] Clark T, Chandrasekhar J. *Isr J Chem* 1993;33:435.